

Oscillations of Bose-Einstein condensates with vortex lattices

II. Finite temperatures

Amen Sedrakian¹ and Ira Wasserman²¹ Institute for Theoretical Physics,
Tubingen University,
D-72076 Tubingen, Germany² Center of Radiophysics and Space Research,
Cornell University, Ithaca,
NY 14853, U.S.A.

Abstract

We derive the finite temperature oscillation modes of a harmonically confined Bose-Einstein condensed gas undergoing rigid body rotation supported by a vortex lattice in the condensate. The hydrodynamic modes separate into two classes corresponding to in-phase (center-of-mass) and counter-phase (relative) oscillations of the thermal cloud and the condensate. The in- and counter-phase oscillations are independent of each other in the case where the thermal cloud is inviscid for all modes studied, except the radial pulsations which couple them because the pressure perturbations of the condensate and the thermal cloud are governed by different adiabatic indices. If the thermal cloud is viscous, the two classes of oscillations are coupled, i.e. each type of motion involves simultaneously mass and entropy currents. The counter-phase oscillations are damped by the mutual friction between the condensate and the thermal cloud mediated by the vortex lattice. The damping is large for the values of the drag-to-lift ratio of the order of unity and becomes increasingly ineffective in either limit of small or large friction. An experimental measurement of a subset of these oscillation modes and their damping rates can provide information on the values of the phenomenological mutual friction coefficients, and hence the quasiparticle-vortex scattering processes in dilute atomic Bose gases.

I. INTRODUCTION

Recent experiments on rotating trapped Bose-Einstein condensates have created vortex lattices with large number of vortices either by stirring a condensate with a rotating anisotropic perturbation [1, 2, 3] or by evaporatively cooling a spinning normal gas [4]. Being reminiscent of the classical rotating bucket experiments, carried out on superfluid phases of Helium, the experiments on rotating Bose-Einstein condensates open a variety of new ways of manipulating a rotating condensate and deducing information on its physical properties, for example, by non-destructive *in situ* imaging [1, 2, 3, 4]. The aspect ratios of the condensates measured in the experiments and the number of vortices deduced from non-destructive imaging are consistent with a rigid body rotation of the condensates. The experiments carried out at finite temperatures [2, 4] achieve a rigid body rotation of the thermal cloud at a frequency close to that of the condensate (for example, in the MIT experiment [2] the ratio of spin-frequencies of the thermal cloud to that of the condensate is close to 2/3). A central theme, motivated by the current experiments, is the oscillations and stability of a Bose condensate that coexists with a rotating thermal cloud and undergoes rigid body rotation supported by a vortex lattice.

In this paper we address the oscillations and stability of a confined, rotating Bose condensate at finite temperatures in the hydrodynamic regime. The angular momentum of the superfluid is carried by singly quantized vortices which form a triangular Abrikosov lattice. We work in the limit of coarse-grained hydrodynamics, where the physical quantities are averages over large number of vortices. In this limit the structure of individual vortices is unresolved and the superfluid simply mimics a rigid body rotation at a frequency $\omega = n_v \hbar / m$, where $\hbar = h/m$ is the quantum of circulation, n_v is the vortex density in the plane orthogonal to the spin vector, m is the boson mass). The hydrodynamic approximation to the microscopic dynamics of the Bose condensate is justified in the regime of strong interparticle interactions and large number of particles in the system (the strong coupling regime requires $N \gg 1$ where N is the net number of particles in the condensate, a is the scattering length, and $d = \hbar/m \omega_0$ is the oscillator length defined in terms of oscillator frequency ω_0). The Thomas-Fermi approximation is valid for systems with large number of particles and insures that quantum corrections (such as the 'quantum pressure' term) to the hydrodynamic equations can be neglected. In addition, for large enough systems the space-local

values of the thermodynamic quantities such as the pressure and chemical potential are well defined. For such systems the coherence length of the condensate $\xi = \frac{p}{8\pi n}$, where n is the number density of the condensate particles, becomes much smaller than the inter-vortex distance and the vortex cores can be treated as singularities in the hydrodynamic equations.

Compared to the zero temperature case the number of degrees of freedom of a Bose condensate is doubled at finite temperatures and so is the number of oscillations modes. The modes can be classified into two subsets, which correspond to the center-of-mass (in-phase) and relative (counter-phase) oscillations of the condensate and the thermal cloud. The first set, which corresponds to density oscillations of the combined uid (first sound), is identical to the modes of a rotating, zero-temperature condensate in the limit of inviscid normal uid and for those modes which do not involve pressure perturbations. These modes were derived within the tensor virial method [5] in a preceding paper [6] (hereafter Paper I). In the special case of an axisymmetric trap, the lowest order non-trivial modes (classified by corresponding terms of the expansion of perturbations in spherical harmonics labeled by indices l, m) are those with $l = 2$ and $m = \pm 2$. Simple analytical results are available in the case of an axisymmetric trap and we list them below for later references. An analysis of the hydrodynamic modes in Ref. [7] of the even m modes belonging to $l = 2$ harmonics is in agreement with the results quoted below. A generalization to odd m and arbitrary $l = 2$ harmonics of the surface modes of a rotating condensate is given in Ref. [8]. The frequencies of the toroidal modes are given by [Paper I, Eq. (34); our notation follows Ref. [5]]

$$\omega_{1,2}(l=2; m=2) = \frac{q}{2!_k^2} \frac{1}{2}; \quad (1)$$

where ω is spin frequency of the condensate, ω_k is the component of the trapping frequency orthogonal to the spin vector; two complementary modes follow from the substitution $\omega_k \rightarrow -\omega_k$.

The frequencies of the pulsation, or breathing, modes are given by [Paper I, Eq. (45)]

$$\omega_{1,2}(l=2; m=0) = \frac{3}{2} \omega_k^2 + 2 \omega_k^2 \frac{q}{9!_k^4} \frac{1}{16(\omega_k^2 + \omega_k^2)^2} \frac{1}{8!_k^2}; \quad (2)$$

where ω_k is the component of the trapping frequency parallel to the spin vector. Finally, the frequencies of the transverse shear modes ($l = 2; m = 1$) are determined by the characteristic equation [Paper I, Eq. (22)]

$$3 \omega_k^2 (\omega_k^2 + \omega_k^2)^2 + 2 \omega_k^2 = 0; \quad (3)$$

There are three distinct modes that solve Eq. (3)

$$s_1 = \frac{2}{3} + (s_+ + s_-); \quad s_{2,3} = \frac{2}{3} - \frac{1}{2}(s_+ + s_-) \pm \frac{\sqrt{3}}{2}(s_+ - s_-); \quad (4)$$

and three complementary modes follow from the substitution $\omega_1 = \omega_2 = \omega_3$ [see Paper I, Eq. (23) and (24)]. (To rewrite the expressions of Paper I in the present notations substitute $\omega_0^2 A_3 = \omega_2^2 A_3 = \omega_k^2$ and specify Eq. (45) for the case of the adiabatic index value $\gamma = 2$. Note that the modes in Paper I are given in a dimensionless form, the frequency unity being ω_0 ; and a normalization is used, $A_1 = 1$, such that ω_0 is identical to the fundamental frequency ω_0). The coefficients in Eqs. (4) are defined as

$$s^3 = \frac{1}{3} \omega_0^2 - 2\omega_k^2 - \frac{\omega_0^2}{9} - \frac{1}{9} \omega_0^4 + \omega_0^2 + \frac{\omega_0^2}{3} \omega_0^2 - 2\omega_k^2 - \frac{\omega_0^2}{9} \omega_0^5 : \quad (5)$$

As we shall see below, Eqs. (1) and (3)–(5) remain valid at finite temperatures when the viscosity of the thermal cloud is negligible; Eq. (2) will be modified since the pulsations of the condensate and the thermal cloud couple due to the difference in the underlying equations of state of these components. In the two-fluid setting these equations correspond to the first class of the in-phase oscillation modes. Note that the oscillation modes quoted above remain valid for non-superfluid Bose or Fermi systems and superfluid Fermi systems at zero temperature. The reason is that the modes are uniquely determined by the assumptions of uniform rotation and harmonic trapping, and by the underlying hydrodynamic equations of motion which are identical for non-superfluid Bose and Fermi fluids and a superfluid Fermi-liquid at zero temperature. [The pulsations of these systems will differ because their equations of states differ, but the corresponding modes can be derived without specifying the value of the adiabatic index, see Eq. (45) in Paper I which applies for arbitrary adiabatic index $\gamma \neq 1$; the $\gamma = 1$ case is treated below].

The purpose of this work is to derive the second class of modes which correspond to the counter-phase oscillations of the condensate and thermal cloud under uniform rotation. We also study in some detail the center-of-mass modes when these are coupled to the relative modes of oscillations. As in the preceding paper we shall use the tensor virial method (Ref. [5] and references therein), however the underlying hydrodynamic equations are now those of the two-fluid superfluid hydrodynamics [9, 10]. Although the tensor virial method was originally developed for the study of equilibrium and stability of uniform, incompressible, rotating liquid masses bound by self-gravitation [5] it proved useful for studies of rotating

Bose-gases confined by harmonic traps. The method was extended to non-uniform compressible flows for gases with polytropic equations of state p / ρ^γ , where p is the pressure, ρ is the density, and γ is the adiabatic index. In this (non-uniform) case the equilibrium figures are heterogeneous ellipsoids of revolution, i.e. ellipsoids with constant density surfaces being similar and concentric to the bounding surface.

This paper is organized as follows. In Sect. 2 we derive the virial equations and their perturbations starting from the two-fluid hydrodynamic equations of strongly correlated, rotating superuids. (Occasionally, we refer to the condensate and the thermal cloud as the superuid and normal uid, respectively). In Sect. 3 we derive the small amplitude first and second order harmonic oscillation modes when the normal uid is inviscid. In the following subsections, the kinematic viscosity of the normal cloud is included in the virial equations and the numerical solutions of the corresponding characteristic equations are presented. Our conclusions are summarized in Section 4. The appendix contains the perturbation equations for the case of anisotropic traps.

II. VIRIAL EQUATIONS AND THEIR PERTURBATIONS

A. Hydrodynamics in a trap

Consider a rotating cloud of Bose condensed gas confined in a harmonic trap. The trapping potential is characterized in terms of Cartesian frequency components ω_i as

$$\omega_{\text{tr}}(\mathbf{x}) = \sum_{i=1}^3 \omega_i^2 x_i^2; \quad (6)$$

we shall assume that the rotation axis is along the z direction of the Cartesian system of coordinates; for axisymmetric traps we set $\omega_1 = \omega_2 = \omega_3$ (hereafter we assume implicit summation over the repeated Latin indices from 1 to 3, unless stated otherwise). The Euler and Navier-Stokes equations for the condensate and the thermal cloud can be combined in a single equation (which is written below in a frame rotating with angular velocity ω relative to some inertial coordinate reference system)

$$\begin{aligned} \frac{\partial}{\partial t} + \mathbf{u} \cdot \nabla \frac{\partial}{\partial \mathbf{x}_j} \mathbf{u}_i = & \frac{\partial p}{\partial x_i} - \frac{1}{2} \frac{\partial \omega_{\text{tr}}}{\partial x_i} + \frac{1}{N} \frac{\partial P_{ik}}{\partial x_k} \\ & + \frac{1}{2} \frac{\partial j}{\partial x_i} \frac{x_j^2}{\partial x_i} + 2 \frac{\partial \mathbf{u}}{\partial x_i} \cdot \mathbf{u} + \mathbf{F}_i; \end{aligned} \quad (7)$$

where the Greek subscripts σ, τ, ν, μ identify the uid component (σ refers to super uid, ν to the normal uid); the Latin subscripts denote the coordinate directions; ρ , p , and u_i are the density, pressure, and velocity of the condensate, P_{ik} is the stress tensor, and $F_{\sigma, i}$ is the mutual friction force on uid σ due to uid ν . Below, we shall assume that the condensate and the thermal cloud are isothermal in the background equilibrium, while the perturbations from the equilibrium state are adiabatic.

The equation of state of the condensate, to the leading order in diluteness parameter $n_s a^3$, where n_s is the number density of condensate atom s , a is the scattering length, can be written in a polytropic form $p_s = K_s n_s$, where K_s is a constant and $\gamma = 2$ is the adiabatic index [6]. The density profile of the condensate in a rotating trap is obtained by integrating Eq. (7) in the stationary (time-independent) limit with respect to the spatial coordinates [Paper I, Eq. (14)]

$$s(x) = s(0) \frac{1}{2K_s} \frac{1}{n(0)^{1/\gamma}} \text{tr}(x) \sum_j x_j^2 ; \quad (8)$$

where $\gamma = 1$ when the expression in the brackets is positive and zero otherwise. The equation of state of the thermal cloud is $p_N(x) = g_{5=2}(z) = g_{3=2}(z) k_B T_N(x)$, where $z = \exp(-k_B T)$ is the fugacity, T is the temperature, k_B is the Boltzmann constant, ϕ is the chemical potential, and $g_h(z) = \prod_{l=1}^h z^{1-l}$; the thermodynamic quantities above refer to local equilibrium values. The density profile of the thermal cloud can be obtained analytically in the temperature and density regime where the quantum degeneracy of the thermal cloud can be neglected. Upon taking the classical limit $z \gg 1$ in the expression for $p_N(x)$, the integration over spatial coordinates leads to

$$N(x) = N(0) \exp \frac{1}{2K_N} \text{tr}(x) \sum_j x_j^2 ; \quad (9)$$

where $K_N = m/k_B T$ and m is the boson mass. Thus, unlike the power-law type profile of the condensate, the density profile of the thermal cloud is Gaussian. While Eq. (8) applies for arbitrary values of the adiabatic index, it is not valid in the special case $\gamma = 1$ occurring for the normal gas in the classical limit. A common feature of the density profiles (8) and (9) is that the centrifugal and trapping potentials are quadratic forms of the coordinates. Thus, the density profiles are generically of the form $s_N = s_N(m^2 s_N)$, where

$$m^2 s_N = \frac{x_1^2}{a_{1,N,s}^2} + \frac{x_2^2}{a_{2,N,s}^2} + \frac{x_3^2}{a_{3,N,s}^2} ; \quad m s_N \ll 1 ; \quad (10)$$

As we shall see below, associated with these density distributions are heterogeneous ellipsoids of the condensate and the thermal cloud with semi-major axis a_{iN} ; ($i = 1, 2, 3$). This observation serves as a starting point for the application of the tensor virial method to describe the equilibrium and stability of ellipsoidal figures of Bose-condensed gases (see also Paper I).

Because of the difference in the equations of state of the condensate and the thermal cloud the underlying hydrodynamic equations [i.e. the components of Eq. (7)] are not invariant with respect to an interchange of the indices labeling the dynamical components (i.e. §).

As a result, the perturbed motions of the components can not be separated into purely in-phase and out-of-phase oscillations for the modes that involve pressure perturbations. The symmetry above is also broken because of the viscosity of the thermal cloud. The Navier-Stokes equation for the normal uid contains the stress tensor in its common form

$$P_{ik} = \eta \left(\frac{\partial u_N}{\partial x_k} + \frac{\partial u_N}{\partial x_i} - \frac{2}{3} \frac{\partial u_N}{\partial x_1} \right)_{ik}; \quad (11)$$

where η is the kinematic viscosity. Thus, we may anticipate that in the inviscid limit and for the modes that do not involve pressure perturbations there are two distinct classes of modes related to the in-phase and out-of-phase oscillations. And these classes mix whenever the modes (e.g. the pulsation modes) require pressure perturbation or the viscosity of the thermal cloud is operative.

Consider the condensate and the thermal cloud rotating uniformly at the same spin frequency; (i.e. we assume the external torque is time-independent and/or the cloud and condensate had sufficient time to relax to a rotational equilibrium). When perturbed from equilibrium theuids interact via the mutual friction force:

$$F_{;i} = S_{ij} \epsilon_{ij} (u_{Sj} - u_{Lj}); \quad (12)$$

where the mutual friction tensor is $\epsilon_{ij} = \epsilon_{ij} + \epsilon_{ijm}^0 + (\epsilon^0)_{ij}$; with ϵ^0 and ϵ^0 being the mutual friction coefficients, $\epsilon_{ij} = \epsilon_{ij} - r_{ij} u_S$ and S is a fully antisymmetric (second rank) unit tensor with the sign convention $S_{SN} = 1$. Note that Eq. (12) is the local form of the mutual friction; when constructing the global (integrated over volume) virial equation we need to take into account the fact that the force acts only within the combined volume of the twouids. Eq. (12) can be put in a form reflecting the balance of forces acting on a vortex

$$S \epsilon_{ijm} (u_{Sj} - u_{Lj})_m - \epsilon_{ij} (u_{Lj} - u_{Sj}) = 0; \quad (13)$$

where $i_{ij} = i_{ij} + i_{ijm}^0 m$, and the components of the friction tensors are related by

$$= \frac{(1 + \theta)}{2 + 1}; \quad \theta = \frac{2 - \theta}{2 + 1}; \quad (14)$$

where $\theta = (s - \theta)$ and $\theta = (s - \theta)$ are the (dimensionless) drag-to-lift ratios. The first term in (13) is a non-dissipative lifting force due to a super flow past the vortex (the Magnus force). The remaining terms reflect the friction between the vortex and the normal fluid. Note that, by definition, work is done only by the component of the friction force θ , which is parallel to the vortex motion. The orthogonal component θ (the Jordansky force) is non-dissipative. While the parallel to the vortex motion component of the friction force has a straight forward micro-physical interpretation in terms of scattering of the normal excitations of the vortex cores, the microscopic nature of the Jordansky force is controversial. We shall include (phenomenologically) this force whenever the results are simple enough to disentangle the effect of a non-zero θ , otherwise we shall set $\theta = 0$. A nonzero θ implies friction along the average direction of the vorticity, which is possible if vortices are oscillating, or are subject to other deformations in the plane orthogonal to the rotation. It is reasonable to assume that for small perturbations the distortions of the vortex lattice are small so that $\theta \ll 1$; $\theta \ll 1$. A peculiar feature of vortex lattice dynamics is the existence of two extreme limits in which the perturbations are weakly damped. In the strong coupling limit ($\theta \ll 1$, at constant θ), when the drag due to the normal fluid dominates, the vortex is locked to the normal fluid and the rearrangements of the lattice, needed for the damping of relative motions between the super fluid and normal fluid, are slow. Similarly, in the weak coupling limit ($\theta \ll 1$, at constant θ) the vortex lattice interacts weakly with the normal fluid, and the perturbations in the normal fluid are transmitted to the vortex lattice and the super fluid on long time scales, i.e. the damping is again ineffective. The damping is largest whenever the interactions of the vortex lattice with super fluid via the Magnus force and the normal fluid via the friction force are of the same order of magnitude ($\theta \ll 1$).

B. Virial equations for uniform rotations

Virial equations of various order are constructed by taking the moments of Eq. (7) with weights $1, x_i, x_i x_j$ etc and integrating over the volume V occupied by the fluid. Taking

the moment of Eq. (7) with weight 1 and integrating over V we obtain

$$\frac{d}{dt} \int_V^Z d^3x \cdot u_{;i} = 2 \int_{\text{im}}^m \int_V^Z d^3x \cdot u_{;1} + (\epsilon^2_{ij} - \epsilon^2_{ii}) I_{;i} \\ - \epsilon_{ij} I_{;j} + \int_V^Z d^3x F_{;i}; \quad (15)$$

where

$$I_{;i} = \int_V^Z d^3x \cdot x_i \quad (16)$$

is the moment of inertia of uid, and we used the boundary condition which assumes that the projection of the stress

$$p_{;ik} + \mathcal{N} P_{ik} = S_{;N}$$

orthogonal to a bounding surface vanishes in equilibrium (the free-surface condition).

Taking the first moment of Eq. (7) with weight x_i and integrating over the volume V results in the second order virial equation

$$\frac{d}{dt} \int_V^Z d^3x \cdot x_j u_{;i} = 2T_{;ij} + \epsilon_{ij} + \mathcal{N} P_{ij} + (\epsilon^2_{ij} - \epsilon^2_{ii}) I_{;ij} \\ + 2 \int_{\text{im}}^m \int_V^Z d^3x \cdot x_j u_{;1} - \epsilon_{ik} I_{;kj} \\ + \int_V^Z d^3x x_j F_{;i}; \quad (17)$$

where

$$I_{;ij} = \int_V^Z d^3x \cdot x_i x_j; \quad T_{;ij} = \frac{1}{2} \int_V^Z d^3x \cdot u_{;i} u_{;j}; \quad P_{ij} = \int_{V_N}^Z d^3x P_{ij}; \quad (18)$$

are the second rank tensors of moment of inertia, pressure, kinetic energy and stress; note that the last tensor is non-zero only in the volume of the thermal cloud.

For uniformly rotating condensate and thermal cloud the stationary second order virial equations define the equilibrium forms of the rotating system; we find

$$\epsilon^2_{ij} (I_{N;ij} - \epsilon_{ij} I_{N;3j}) - \epsilon^2_{ii} I_{N;ij} = \epsilon_{ij} N; \quad (19)$$

$$\epsilon^2_{ij} (I_{S;ij} - \epsilon_{ij} I_{S;3j}) - \epsilon^2_{ii} I_{S;ij} = \epsilon_{ij} S; \quad (20)$$

where the mixture rotates about the x_3 axis. The diagonal components of these equations provide the equilibrium ratios of the components of the moment of inertia tensor

$$\frac{I_{N;33}}{I_{N;11}} = \frac{I_{S;33}}{I_{S;11}} = \frac{\epsilon^2_1 - \epsilon^2_3}{\epsilon^2_3}; \quad (21)$$

$$\frac{I_{N,33}}{I_{N,22}} = \frac{I_{S,33}}{I_{S,22}} = \frac{!_2^2}{!_3^2} : \quad (22)$$

The moment of inertia tensor of a heterogeneous ellipsoid is

$$I_{ij} = \frac{4}{3} a_i^3 a_j a_k a_l \int_0^{Z_1} (m^2) m^4 dm ; \quad (23)$$

where the density distributions (m^2) are defined in Eqs. (8) and (9). The total mass in the uid can be related to the moment of inertia tensor by noting that

$$M = 4 a_1 a_2 a_3 \int_0^{Z_1} (m^2) m^2 dm : \quad (24)$$

Using Eq. (23) in Eqs. (21) and (22) we find the ratios of the semi-axes in the equilibrium

$$\frac{a_{N,3}}{a_{N,1}} = \frac{a_{S,3}}{a_{S,1}} = \frac{!_1}{!_3} 1 \frac{!_2^2}{!_1^2} ; \quad (25)$$

$$\frac{a_{N,3}}{a_{N,2}} = \frac{a_{S,3}}{a_{S,2}} = \frac{!_2}{!_3} 1 \frac{!_2^2}{!_2^2} ; \quad (26)$$

Despite of the difference in the density profiles of the condensate and the thermal cloud the semi-axis ratios (but not the semi-axis themselves!) are equal; they depend only on the rotation rate and hence are the same for corotating uids. For axially symmetric gures these conditions place an upper limit on the rotation frequency $< !_2$. In the non-axisymmetric case $< m \min(!_1, !_2)$ for xed $!_1$ and $!_2$ or, alternatively, $!_2 >$ for xed $!_1$ at $< !_1$. Note that these boundaries correspond to stable solutions under stationary conditions and within the ellipsoidal approximation. Perturbations away from the stability region can results in either dynamically unstable gures that preserve their ellipsoidal structure or (stable) con gurations that are not ellipsoids (e.g. the Poincaré's pear-shaped gures) [5].

C. Perturbation equations for uniform rotations

Consider small perturbations from the equilibrium state of uniformly rotating condensate and thermal cloud. Eulerian variations of the rst order virial equation lead to

$$f \frac{d^2 V_{,i}}{dt^2} = 2 \lim_m \frac{d}{dt} V_{,i} + (\frac{2}{2} \frac{d}{dt} V_{,ij} - \frac{d}{dt} V_{,ij}) f V_{,j} - f !_i^2 V_{,i} \\ (1 -) f_s !_s \frac{d}{dt} \hat{V}_{,ij} - \hat{V}_{,ij} : \quad (27)$$

The variations of the second order virial equation give

$$f \frac{d^2 V_{,ij}}{dt^2} = 2 \sum_m f \frac{dV_{,ij}}{dt} + (1 - f_s) \sum_k \frac{d}{dt} \hat{V}_{,kj} - \hat{V}_{,kj} + \sum_{ij} P_{ij}; \quad (28)$$

where $f = \frac{m}{M}$ is the fraction of the mass in the uid, P_{ij} is the Eulerian variation of the stress tensor, and the virials $V_{,i}$, $V_{,ij}$ are defined in terms of the Lagrangian displacement as

$$V_{,i} = \frac{1}{Z} \int_V d^3 x_{,i}; \quad (29)$$

$$V_{,ij} = \frac{1}{V} \int_V d^3 x_{,i} x_{,j}; \quad (30)$$

and $V_{,ij} = V_{,ji} + V_{,j,i}$. The volume integration over the terms corresponding to the mutual friction must be carried out over the overlap volume of the two uids, since in general the uids do not occupy the same volume in the background equilibrium. The modified virials

$$\hat{V}_{,ij} = (1 - f_N) V_{,ij}; \quad (31)$$

in Eqs. (27) and (28) take this feature into account in terms the volume reduction factor $f > 0$; the sign of f in Eq. (31) corresponds to the case where the condensate is embedded in a thermal cloud of a larger volume, as is frequently the case in experiments. Eqs. (27) and (28) assume that the density gradients are smooth enough to allow for averaging of the mutual friction coefficients over the cloud. [It is not possible to derive strict criteria for the validity of the density average approximation for the mutual friction (or other related kinetic) coefficients unless one identifies a particular mechanism of scattering of the thermal excitations of the vortices].

The center-of-mass and relative motions of the uid can be decoupled by defining new linear combinations of the virials

$$V_{ij} := f \hat{V}_{s,ij} + f_N \hat{V}_{N,ij}; \quad (32)$$

$$U_{ij} := \hat{V}_{s,ij} - \hat{V}_{N,ij}; \quad (33)$$

The decoupling is perfect when the hydrodynamic equations of the uids (7) are symmetric/anti-symmetric with respect to an exchange of the indices labeling the uids. This is the case for the first order equations (due to the surface boundary conditions). For

the second order equations the symmetry is broken by either the difference in the pressure perturbations of the condensate and the thermal cloud or by the viscosity which acts only in the normal gas. Nevertheless, we proceed to rewrite the original equations (27) and (28) in terms of the new virials (32) and (33) even though in a number of cases the modes related to these virials will be mixed.

At the first order the center-of-mass motions of the two-uids are trivial, since they can be eliminated by a linear transformation to the reference frame where $V_i = 0$. The center-of-mass modes of second order are governed by the equation

$$\frac{d^2 V_{ij}}{dt^2} = 2 \frac{dV_{ij}}{dt} + (2 - !_i) V_{ij} - i_k V_{kj} + ij^{(+)}; \quad (34)$$

which differs from Eq. (11) of Paper I by the form of the perturbation of the stress tensor $^{(+)} = [(1 -)_N + s]$. Consequently, all the second harmonic modes contained in Eq. (34) are identical to those derived in Paper I [see also Eqs. (1)–(4)] except the quasi-radial pulsation modes, which require the explicit form of the pressure tensor. We shall return to these modes, since they do involve a mixing of the center-of-mass and relative motions and differ from those in Paper I. The first and second order virial equations for the counter-phase motions are

$$\frac{d^2 U_i}{dt^2} = 2 \frac{dU_i}{dt} + (2 - !_i) U_i - i_j U_j - !_s \tilde{ij} \frac{dU_j}{dt}; \quad (35)$$

$$\frac{d^2 U_{ij}}{dt^2} = 2 \frac{dU_{ij}}{dt} + (2 - !_i) U_{ij} - i_k U_{kj} + ij^{(+)} - 2 \tilde{ik} \frac{d}{dt} U_{kj}; \quad (36)$$

where $\tilde{ij} = [1 + (1 -)_N f_N^{-1}]_{ij}$ and $^{(+)} = f_s^{-1} s - f_N^{-1} (1 -)_N$: The first of these relations simply re-scales the mutual friction coefficients to account for the absence of condensate fraction in the exterior of the cloud: in the limit of coinciding volumes ($= 1$) the two coefficients are identical. The second relation implies that the resulting pressure perturbations that couple the two-uid relative motions to the center-of-mass motions are proportional to the difference in the perturbations of the individual uids weighted by their fraction in the total volume. Note that the constants entering the relation for $^{(+)}$ can be chosen such as to eliminate the pressure perturbation from the virial equation (36); in this special case the modes derived from the virial equations would correspond to those of an inviscid uid.

III. SMALL AMPLITUDE OSCILLATIONS

We assume the time-dependence of Lagrangian displacements of the condensate and the normal uid are of the form

$$(x_i; t) = (x_i) e^{i \omega t}; \quad (37)$$

When these Lagrangian displacements are substituted in the definitions of the virials, Eqs. (35) and (36) provide a set of characteristic equations that determined the modes associated with the first and second order moments of the hydrodynamic equations (the first and second order virial equations). We turn now to the characteristic equations that derive from the virial equations (35) and (36).

A. First order oscillations

The characteristic equation for the first order relative oscillation modes is

$$\omega^2 + \omega_1^2 U_i + 2i \omega_m U_1 \omega_{ij} + 2i \omega_{ij} U_j = 0; \quad (38)$$

The components of Eq. (38) along and orthogonal to the rotation axis (i.e. those with odd and even parity with respect to inversions of the z-direction) decouple. We find, respectively,

$$\omega_{\text{odd}} = \frac{q}{\omega_1^2 + \omega_m^2} \omega_1^2; \quad (39)$$

$$\omega_{\text{even}} = (1 - \omega_1^2) + i \sqrt{X^2 + Y^2} e^{i \omega_1 t}; \quad (40)$$

where $X = \omega_1^2 + \omega_m^2 - 2\omega_1^2$, $Y = 2\omega_1(1 - \omega_1^2)$ and $\tan \theta = Y/X$. The odd parity modes are stable and damped; note that if $\omega_1^2 > \omega_m^2$ the modes are purely imaginary. The asymptotics of the even parity modes, neglecting the rescaling of the coefficients due to the mismatch of the volumes of uids is as follows. For small we find

$$\text{Re } \omega = (1 + \omega_1^2)^{1/2} + O(\omega_1^2); \quad (41)$$

$$\text{Im } \omega = (1 + \omega_1^2)^{1/2} (1 + \omega_1^2)^{1/2} = \omega_1^2 + O(\omega_1^3); \quad (42)$$

where $\omega_1^2 = \omega_1^2 + \omega_m^2 (1 + \omega_1^2)^2$; for large ω_1 , we find

$$\text{Re } \omega = \frac{q}{\omega_1^2 + \omega_m^2} \omega_1^2 + O(\omega_1^2); \quad (43)$$

$$\text{Im } \omega = (1 + \omega_1^2)^{1/2} = \omega_1 + O(\omega_1^3); \quad (44)$$

Eqs. (41)–(43) are written at the zeroth order of the expansion with respect to the small parameter $\epsilon = (\zeta^0 - \zeta^0) = 0$, which re-scales the coefficients due to the mismatch of volumes of the voids. The ratios of the real to the imaginary part of the modes increase linearly in both, the strong and weak coupling limits for fixed ζ^0 , hence the modes are weakly damped in both limits. An exception is the strong-coupling limit when $\zeta^0 / \zeta^0 \rightarrow 0$, in which case the ratio of the real to the imaginary part tends to a constant value $\zeta^0 / \zeta^0 \rightarrow \zeta^0 / \zeta^0 = 1$.

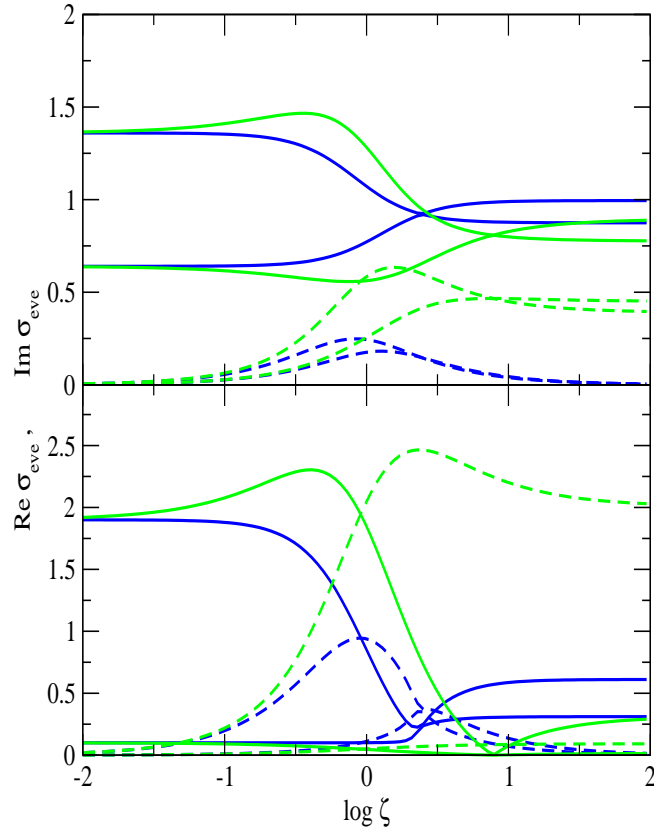


FIG. 1: The real (solid lines) and imaginary (dashed lines) parts of the first order even-parity modes as functions of the drag-to-lift ratio $\log \zeta$. The blue (heavy) and the green (light) lines correspond to $\zeta^0 = 0$ and $\zeta^0 = 0.9$ cases. The upper and lower panels correspond to the rotation frequencies $\Omega = 0.36$ and $\Omega = 0.9$, respectively. The frequencies are in units of ζ^0 .

The real (solid lines) and imaginary (dashed lines) parts of the first order even-parity modes as functions of the drag-to-lift ratio $\log \zeta$ are shown in Fig. 1. The frequencies are in units

of $!_?$. The parameter values correspond to the recent MIT experiment [2]: $!_3^2 = !_?^2 = 0.057$, $f_S = 0.2$, $f_N = 0.8$ and we assumed that the overlap volume corresponding to $= 0.5$. The two panels in Fig. 1 are representative for the slow and fast rotation limits. The modes in the upper panel were computed for the spin frequency $= !_? = 0.36$ (as is the case in the experiment [2]); the modes in the lower panel were computed for a near critical spin frequency $= !_? = 0.9$. The heavy (blue) and light (green) lines correspond to the cases $^0 = 0$ and $= 0$, respectively. The generic features of the modes (seen also for more complicated cases below) are the asymptotically constant values of the real and the vanishing of the imaginary parts, except for the case of $= 0$ and strong coupling ($= 1$) where the damping tends to a constant value asymptotically. The mode crossing occurs when the condition $\sim^0 = 1$ is fulfilled. This can be seen directly from the characteristic equations: the real and imaginary parts degenerate to a single value since the first term on right hand side of Eq. (40) and the phase of the second term in Eq. (40) are zero for $\sim^0 = 1$. The position of the mode crossing when $= 0$ and $= 0$ is different. The reason is that while the mode crossing is still defined by the condition $\sim^0 = 1$, the functional dependence of 0 on \sim^0 for $= 0$ and $= 0$ changes. One of the imaginary parts has its maximum at the position of the crossing, the other maximum is at $= 1$.

In the weak coupling limit ($= 1$) the splitting in the real parts of the modes is twice the rotation frequency consistent with Eq. (41) and the centroid is at $\text{Re } \omega_{\text{eve}} = !_?$. In the strong coupling limit ($= 1$) the splitting would have been absent if theuids were to occupy the same volume (i.e. $^0 = \sim^0 = 1$ when $!_? = 1$). Writing $\sim^0 = (1 -)^0$ [see the first relation after Eq. (36)] the modified strong coupling expansion (43) to next-to-leading order in $= 1$ reads

$$\text{Re } !_? \frac{^0}{!_?^2 - \sim^0} + \mathcal{O}(\sim^0) + \mathcal{O}(\sim^0^2): \quad (45)$$

Thus, the splitting of the real parts of the modes in the strong coupling regime is a direct measure of the renormalization, \sim^0 , of the coefficient due to the mismatch of the volumes of the condensate and the thermal cloud. The centroid of the splitting is defined by the first term in Eq. (45). The overall behaviour of the modes in the fast (or near critical, $= !_? = 1$) rotation regime, shown in the lower panel of Fig. 1, is the same as for the slow rotations. The splittings of the real parts of the modes are magnified in the strong and weak coupling limits, since these scale linearly with $= 1$. Unlike the slow rotation regime, the modes are

either partially (for $\alpha = 0$) or fully (for $\alpha = \pi$) damped in the strong coupling limit. Note that the point where the modes cross is independent of α (and is the same in the upper and lower panels).

The analysis above shows that the first order even-parity modes associated with the relative (or out-of-phase) motions of the condensate and the thermal cloud contain rich information on the physics of a rotating condensed Bose gas. The values of the phenomenological mutual friction coefficients, the fractional volumes occupied by the constituents, and related parameters can be deduced by mapping out the functional dependence of the modes on the rotation frequency and friction. The friction can be varied by manipulating the strength of the interaction among the particles. The odd-parity counterparts, although trivial, could provide information on the deviations of the flow and vortex lattices from the axial symmetry about the spin axis. If deviations are observed in the odd-parity modes from the value of z-component of the trapping frequency and/or there is an evidence of their damping, this would indicate non-zero friction orthogonal to the equatorial plane, which could be caused, for example, by convective motions or vortex bending.

B. Second order harmonic oscillations

1. Inviscid limit

It is instructive to consider the second-order harmonic small-amplitude oscillations first in the inviscid limit ($\alpha = 0$). The characteristic equations for the second order center-of-mass and relative oscillations modes are

$$^2V_{ij} + (^2 - !_i^2) V_{ij} + 2i \sum_m V_{lj} - i \sum_k V_{kj} + \epsilon_{ij}^{(+)} = 0; \quad (46)$$

$$^2U_{ij} + (^2 - !_i^2) U_{ij} + 2i \sum_m U_{lj} - 2i \sum_k U_{kj} + \epsilon_{ij}^{(-)} = 0; \quad (47)$$

The even- and odd-parity modes can be treated separately. Eq. (46) for center-of-mass oscillations differs from the analogous Eq. (11) of Paper I by the variation of the stress tensor; since the transverse-shear ($l=2$ and $j=1$) and the toroidal ($l=2$ and $j=2$) modes do not involve this quantity, these modes are identical to those derived earlier, see Eqs. (1) and (4). The quasi-radial pulsation modes do mix for the center-of-mass and

relative oscillations and will be examined below.

We start with the remaining toroidal and transverse-shear modes of relative oscillations.

The first set of modes is governed by the equations

$$h^2 + 2i\tilde{\omega} + 2(\lambda_?^2)^{\frac{1}{2}}(U_{11} - U_{22}) - 4i(1 - \tilde{\omega}^0)U_{12} = 0; \quad (48)$$

$$h^2 + 2i\tilde{\omega} + 2(\lambda_?^2)^{\frac{1}{2}}U_{12} + i(1 - \tilde{\omega}^0)(U_{11} - U_{22}) = 0; \quad (49)$$

The associated characteristic equation and the solutions are identical to Eq. (39) and (40), respectively, if we replace the radial trapping frequency in these equations by $\lambda_?^2 = 2\lambda_?^2$; clearly, with the substitution above, the limiting behavior of the modes for large and small frictions are the same as for the first order harmonic modes. The transverse-shear (odd parity) modes are given by the components of Eq. (47) for the irreducible set of tensors $U_{i;3}$ and U_{i3} , $i = 1, 2$:

$$(\lambda^2 + 2i\tilde{\omega})U_{1;3} - 2i(1 - \tilde{\omega}^0)U_{2;3} + (\lambda_?^2)^{\frac{1}{2}}U_{13} = 0; \quad (50)$$

$$(\lambda^2 + 2i\tilde{\omega})U_{2;3} + 2i(1 - \tilde{\omega}^0)U_{1;3} + (\lambda_?^2)^{\frac{1}{2}}U_{23} = 0; \quad (51)$$

$$(\lambda^2 - 2i\tilde{\omega}^0)U_{1;3} + (\lambda^2 + 2i\tilde{\omega}^0 + \lambda_3^2)U_{13} = 0; \quad (52)$$

$$(\lambda^2 - 2i\tilde{\omega}^0)U_{2;3} + (\lambda^2 + 2i\tilde{\omega}^0 + \lambda_3^2)U_{23} = 0; \quad (53)$$

The corresponding characteristic equation is of order seven and will not be written down; we shall return to the numerical solution of the characteristic equation in a later subsection.

As pointed out above, the center-of-mass and relative quasi-radial oscillations modes are coupled due to the difference in the perturbations of the stress tensor of the condensate and the thermal cloud. We now express these perturbations in terms of the virials V_{ij} and U_{ij} . The Eulerian perturbation for the condensate has been derived earlier [Paper I, Eq. (42)]

$$s = \frac{1}{2}h(\lambda_?^2)^{\frac{1}{2}}(V_{S;11} + V_{S;22}) + \lambda_3^2 V_{S;33}; \quad (54)$$

where $\lambda = 2$ for the condensate. A diabatic perturbations of the thermal cloud leave the quantity p_N unchanged. For the perturbation of the stress tensor of the thermal cloud we find

$$_N = \int_{V_N}^Z (p_N + p_N r_N) d^3x = \frac{2}{3} \int_{V_N}^Z r_N p d^3x; \quad (55)$$

where we used the relation between the Eulerian () and Lagrangian () variations: $\lambda = r + r$. The gradient of the pressure p is computed from the equilibrium limit of the

Navier-Stokes equation (7). We find

$$N = \frac{1}{2} \frac{^0h}{2} (!_?^2 - ^2) (V_{N,11} + V_{N,22}) + !_3^2 V_{N,33}^i; \quad (56)$$

where the effective adiabatic index is $^0 = 5/3$. Note that the adiabatic index governing the perturbations need not be identical to the one that governs the equilibrium background, as is the case for the thermal cloud. Using Eqs. (54) and (56) we find

$$^{(+)} = \frac{1}{2} (1 - \frac{^0}{f_N} - \frac{^h}{f_S}) (V_{11} + V_{22}) (!_?^2 - ^2) + V_{33} !_3^2 \quad (57)$$

$$^{(-)} = \frac{1}{2} (1 - \frac{^0}{f_S} - \frac{^h}{f_N}) (U_{11} + U_{22}) (!_?^2 - ^2) + U_{33} !_3^2 \quad (58)$$

Note that if $\gamma = 0$ the $^{(-)}$ variations vanish. By a suitable combination of the even-parity components of Eq. (46) we find the following set of equations for the virial combinations $V_{11} + V_{22}$, $V_{1,1} - V_{2,1}$ and V_{33}

$$^2 = 2 !_?^2 + ^2 (V_{11} + V_{22}) - 2i (V_{1,2} - V_{2,1}) - ^2 2 !_3^2 V_{33} = 0; \quad (59)$$

$$^2 (V_{1,2} - V_{2,1}) + i (V_{11} + V_{22}) = 0; \quad (60)$$

$$(^2 - 2 !_3^2) V_{33} + 2 ^{(+)} = 0; \quad (61)$$

where $^{(+)}$ Eq. (57) involves the same set of virials and, in addition, couples these equations to the virials describing relative motions. Analogous manipulations on Eq. (47) lead to

$$^2 = 2 i \sim !_?^2 + ^2 (U_{11} + U_{22}) - ^2 2i \sim^0 2 !_3^2 U_{33} - 2i (1 \sim^0) (U_{1,2} - U_{2,1}) = 0; \quad (62)$$

$$(^2 - 2i \sim) (U_{1,2} - U_{2,1}) + i (1 \sim^0) (U_{11} + U_{22}) = 0; \quad (63)$$

$$(^2 - 4i \sim^0 - 2 !_3^2) U_{33} + 2 ^{(-)} = 0; \quad (64)$$

with $^{(-)}$ defined by Eq. (58). The corresponding characteristic equations for the quasi-radial pulsation modes ($l=2, m=0$) is of order nine. The numerical solutions are given in subsection C.

2. Including viscosity of thermal cloud

The variations of the stress-tensor Eq. (11) can not be expressed in terms of virials in general. This can be done, however, in the perturbative regime, when the effects of viscosity are small (the criterion for the validity of the perturbation theory is discussed in the next subsection). The variation of the stress-energy tensor in the background equilibrium without internal motions ($u = 0$) is

$$P_{ij} = \int_{V_N}^Z \left(\frac{\partial}{\partial t} \frac{\partial_{N;j}}{\partial x_i} + \frac{\partial_{N;i}}{\partial x_j} - \frac{2}{3} \frac{\partial_{N;1}}{\partial x_1} \right)_{ij} d^3x; \quad (65)$$

and the last term vanishes for incompressible fluids. Eq. (65) assumes that the kinematic viscosity can be replaced by its average over the profile of the normal cloud, in line with the similar assumption about the mutual friction coefficients.

The perturbative approach expresses the stress-energy tensor in terms of Lagrangian displacements corresponding to the inviscid limit (see, e.g., [5]). Quite generally, these can be written as

$$N_{;i} = L_{N;i;j} x_j \quad (66)$$

where $L_{N;i;j}$ are nine unknowns which are determined from the solution of the virial equations of second order in the inviscid limit [no summation over the repeated indices in Eq. (66)]. Using Eqs. (37), (66) in (65) we obtain

$$P_{ij} = \int_{V_N}^Z \left(L_{N;i;j} + L_{N;j;i} - \frac{2}{3} L_{N;1;1} \right)_{ij} d^3x; \quad (67)$$

On the other hand, noting that the moment of inertia tensor of a heterogeneous ellipsoid is diagonal, we find

$$\int_{V_N}^Z L_{N;i;j} x_j d^3x = L_{N;i;i} I_{N;j;j}; \quad (68)$$

(no summation over the repeated indices). Next using the expressions for the moment of inertia tensor and the mass of heterogeneous ellipsoids, Eqs. (23) and (24), we write the ratio $I_{N;i;i}/M_N = a_i^2 = 5$, where

$$a_i^2 = 5 \int_0^1 \int_{V_N}^Z (m_N^2) m_N^4 dm_N \quad 3 \int_0^1 \int_{V_N}^Z (m_N^2) m_N^2 dm_N \quad 1 : \quad (69)$$

Then, Eq. (67) becomes

$$P_{ij} = 5 \int_{V_N}^Z \left(\frac{V_{N;i;j}}{a_j^2} + \frac{V_{N;j;i}}{a_i^2} - \frac{V_{N;1;1}}{3a_1^2} \right)_{ij} d^3x : \quad (70)$$

The final form of the equations governing the small amplitude oscillations in the viscous fluid will contain only the ratios of the semi-axes of the ellipsoids and a renormalized value of the kinematic viscosity; therefore instead of evaluating the expression (69), the relations (26) will be used. On substituting Eq. (67) in Eqs. (46) and (47) we find

$${}^2V_{ij} = 2i \text{ if}_N V_{1;j} + ({}^2 - !_i^2)V_{ij} - i_k V_{kj} + ij^{(+)} \\ 5i \text{ if}_N \frac{V_{ij}}{a_j^2} + \frac{V_{j;i}}{a_i^2} - \frac{V_{11}}{3a_1^2} ij + 5i \text{ if}_N f_S \frac{U_{ij}}{a_j^2} + \frac{U_{j;i}}{a_i^2} - \frac{U_{11}}{3a_1^2} ij ; \quad (71)$$

$${}^2U_{ij} = 2i \text{ if}_N U_{1;j} + ({}^2 - !_i^2)U_{ij} - i_k U_{kj} + ij^{(+)} - 2i \text{ if}_N U_{kj} \\ + 5i \text{ if}_N \frac{V_{ij}}{a_j^2} + \frac{V_{j;i}}{a_i^2} - \frac{V_{11}}{3a_1^2} ij - 5i \text{ if}_N \frac{U_{ij}}{a_j^2} + \frac{U_{j;i}}{a_i^2} - \frac{U_{11}}{3a_1^2} ij ; \quad (72)$$

Eqs. (71) and (72), which (if written in components) constitute a coupled set of eighteen equations, contain all the second harmonic modes which correspond to surface deformations with $l=2$ and $m=2$ indices of the expansion in the spherical harmonics. The equations with odd and even parity with respect to the index 3 decouple for linear perturbations and can be treated separately.

The transverse shear modes are determined by the eight components of the Eqs. (71) and (72) which are odd in index 3, i.e. $V_{3;i}$, $V_{i;3}$, $U_{3;i}$ and $U_{i;3}$, where $i=1;2$. The odd equations for the virials describing the center-of-mass motions are

$${}^2 \text{ if}_N V_{1;3} + !_3^2 V_{13}^2 + \text{ if}_N V_{13} - 2i V_{2;3} \\ \text{ if}_N f_S U_{13} + \text{ if}_N f_S U_{1;3} = 0; \quad (73)$$

$${}^2 \text{ if}_N V_{2;3} + !_3^2 V_{23}^2 + \text{ if}_N V_{23} + 2i V_{1;3} \\ \text{ if}_N f_S U_{23} + \text{ if}_N f_S U_{2;3} = 0; \quad (74)$$

$${}^2 + \text{ if}_N + !_3^2 V_{13}^2 + \text{ if}_N V_{1;3} \\ \text{ if}_N f_S U_{13} + \text{ if}_N f_S U_{1;3} = 0; \quad (75)$$

$${}^2 + \text{ if}_N + !_3^2 V_{23}^2 + \text{ if}_N V_{2;3} \\ \text{ if}_N f_S U_{23} + \text{ if}_N f_S U_{2;3} = 0; \quad (76)$$

where $!_3^2 = a_3^2$ and we defined the kinematic viscosity as $\eta^0 = 5 = a_1^2$ and dropped the prime in the equations above. The relations $V_{ij} = V_{i;j} + V_{j;i}$ and $U_{ij} = U_{i;j} + U_{j;i}$, which relate the virials that are symmetric and non-symmetric in their indices have been used to manipulate the components of Eq. (71) to the form above. For the virials describing the

relative motions the odd parity equations are

$$^2 + 2i \sim \text{if} \quad U_{1;3} + !^2_? \quad ^2 + \text{if}_S \quad U_{13} \quad 2i (1 \sim^0) U_{2;3} \\ + i \quad V_{1;3} \quad i \quad V_3 = 0; \quad (77)$$

$$^2 + 2i \sim \text{if} \quad U_{2;3} + !^2_? \quad ^2 + \text{if}_S \quad U_{23} + 2i (1 \sim^0) U_{1;3} \\ + i \quad V_{2;3} \quad i \quad V_3 = 0; \quad (78)$$

$$^2 + 2i \sim^0 + !^2_3 + \text{if}_S \quad U_{13} \quad ^2 + 2i \sim^0 + \text{if}_S \quad U_{1;3} \\ i \quad V_3 + i \quad V_{1;3} = 0; \quad (79)$$

$$^2 + 2i \sim^0 + !^2_3 + \text{if}_S \quad U_{23} \quad ^2 + 2i \sim^0 + \text{if}_S \quad U_{2;3} \\ i \quad V_3 + i \quad V_{2;3} = 0; \quad (80)$$

The two sets (73)–(76) and (77)–(80) decouple in the limit $! \rightarrow 0$, as they should. The dissipation in the first set is driven by the viscosity of the normal matter. In the second set the normal matter viscosity contributes to the damping of the Lagrangian displacements which are orthogonal to those damped by the mutual friction, and in addition, there is a linear renormalization of the mutual friction damping time scale $2 \sim ! 2 \sim + (1 \sim) \text{if}$. Note that this renormalization vanishes for a sphere, since then $! = 1$. The characteristic equation resulting from the set of Eqs. (73)–(80) is of order twelve.

The toroidal modes are determined by the even in index 3 components of Eqs. (47) and (46) written for the virials $V_{i;i}$, $V_{i;j}$, $U_{i;i}$ and $U_{i;j}$, where $i, j = 1, 2$. These equations can be manipulated to a set of four equations, which read

$$^h \quad ^2 + 2(!^2_? \quad ^2) + 2\text{if}_N \quad ^i (V_{11} \quad V_{22}) \quad 4i \quad V_{12} \\ 2\text{if}_N \text{f}_S \quad (U_{11} \quad U_{22}) = 0; \quad (81)$$

$$^h \quad ^2 + 2(!^2_? \quad ^2) + 2\text{if}_N \quad ^i V_{12} + i \quad (V_{11} \quad V_{22}) \\ 2\text{if}_N \text{f}_S \quad U_{12} = 0; \quad (82)$$

$$^h \quad ^2 + 2i \sim + 2\text{if}_S \quad + 2(!^2_? \quad ^2) \quad ^i (U_{11} \quad U_{22}) \quad 4i (1 \sim^0) U_{12} \\ 2i \quad (V_1 \quad V_2) = 0; \quad (83)$$

$$^h \quad ^2 + 2i \sim + 2\text{if}_S \quad + 2(!^2_? \quad ^2) \quad ^i U_{12} + (1 \sim^0) i \quad (U_{11} \quad U_{22}) \\ 2i \quad V_2 = 0; \quad (84)$$

As above, the effect of the kinematic viscosity is the coupling of the center-of-mass and

relative modes and the renormalization of the damping due to the mutual friction $\sim !$
 $\sim + f_s$. The corresponding characteristic equations is of eighth order.

The pulsation modes are determined by the equations which are even in index 3. For incompressible ellipsoids these should be supplemented by the conditions of vanishing of the divergence of perturbations of each uid [Paper I, Eq. (38) and its analog for the U_{ii} virials]. We shall proceed directly to the compressible uid case. By suitable combination of the equations for the virials $V_{i,j}$, $V_{i,j}$, $U_{i,j}$ and $U_{i,j}$, where $i = 1, 2, 3$ and $j = 1, 2$ the initial set of equations can be reduced to

$$\frac{2}{2} + if_N + !_3^2 \stackrel{!}{h} (V_{11} + V_{22}) + 2i (V_{1,2} - V_{2,1}) \quad (85)$$

$$2f_N^2 (1 -)i + 2!_3^2 V_{33} \quad (86)$$

$$if_N f_s (U_{11} + U_{22}) - 2if_N f_s (1 -) U_3 = 0; \quad (87)$$

$$" \quad \stackrel{!}{h} (V_{1,2} - V_{2,1}) - i (V_{11} + V_{22}) = 0; \quad (88)$$

$$\frac{2}{2} + \frac{2i}{3} (1 -)f_N + !_3^2 V_{33} - \frac{i}{3} f_N (V_{11} + V_{22}) \quad (+) \\ \frac{2i}{3} (1 -)f_N f_s U_{33} + \frac{i}{3} f_N f_s (U_{11} + U_{22}) = 0; \quad (89)$$

$$\frac{2}{2} + if_s + i \sim + !_3^2 \stackrel{!}{h} (U_{11} + U_{22}) + 2i (1 - \sim^0) (U_{1,2} - U_{2,1}) \\ 2 + 2i \sim^0 + 2!_3^2 + 2if_s (1 -) U_{33} \\ i (V_{11} + V_{22}) - 2i (1 -) V_3 = 0; \quad (90)$$

$$" \quad (\stackrel{!}{h} + 2i \sim) (U_{1,2} - U_{2,1}) - i (1 - \sim^0) (U_{11} + U_{22}) = 0; \quad (91)$$

$$\frac{2}{2} + \frac{2i}{3} (1 -)f_s + i \sim^0 + !_3^2 U_{33} - \frac{i}{3} f_s (U_{11} + U_{22}) \quad () \\ \frac{2i}{3} (1 -) V_3 + \frac{i}{3} (V_{11} + V_{22}) = 0; \quad (92)$$

where $(+)$ and $()$ are defined in Eqs. (57) and (58). Note that the role of kinematic viscosity is to renormalize the damping along the spin axis as $\sim^0 ! - \sim^0 + f_s (1 -)$ and in the plane orthogonal to the spin axis as $\sim ! - \sim + f_s$. The characteristic equation is of order nine.

The perturbation expansion with respect to the inviscid limit requires $1 \rightarrow 0$, where 1 and 0 are the modes in the viscous and inviscid limits. Since the characteristic equations which include uid viscosity do not permit analytical solutions in general, the validity of the

perturbation expansion can be checked numerically (*a posteriori*) by comparing the values of α_0 and α_1 for a fixed mode. Another expansion parameter, that enters only the equations for the relative virials is $\beta = 1$; the latter condition insures that the modulations of the damping of the modes due to the viscosity are small compared to the inviscid but dissipative (due to the mutual friction) case.

C. Numerical solutions

We now turn to the numerical solutions of the characteristic equations for the second order virials. The parameter values used below are the same as those for the first order oscillation modes. The upper and lower panels in figures below show the results for the slow ($\omega = 0.36$) and fast ($\omega = 0.9$) rotation limits, respectively. The black (heavy) lines correspond to the inviscid case with $\beta = 0$; the orange (medium light) lines correspond to the inviscid case but with $\beta = 1$, and the green (light) lines – to the viscous normal uid case with $\beta = 0$. The coefficient β^0 is set equal zero everywhere.

Fig. 2 shows the real (solid lines) and imaginary (dashed lines) parts of the second order transverse-shear modes ($l = 2; m = \pm 1$). The characteristic equation for the transverse-shear modes is of order seven, however the solutions appear as complex conjugate pairs, i.e. there are only three distinct solutions plus a zero-frequency mode; this mode degeneracy reflects the axial symmetry of the problem. We start the discussion with the inviscid limit. When $\beta^0 = 0$, the real and imaginary parts of the two high-frequency modes coincide while the real part of the third low-frequency mode vanishes for $\beta^0 = 1$. The mode-crossing can be traced back to the fact that the terms $1/\beta^0$ in Eqs. (50) and (51) vanish and the underlying equations become invariant under the exchange of the indices 1 and 2. Non-zero β^0 causes a shift in the value of β where the modes cross, which is a simple consequence of the different functional dependence of β on β^0 for the cases $\beta^0 = 0$ and $\beta^0 = 1$. Note that the crossover from the weak to the strong coupling regime is monotonic for the case $\beta^0 = 0$ while the functions acquire maximum or minimum at intermediate values of β when $\beta^0 \neq 0$. The asymptotics of the real and imaginary parts of the transverse-shear modes are the same as for the first order even-parity modes (Fig. 1): the real parts of the modes tend asymptotically to constant values and the imaginary parts vanish except for the case of $\beta = \beta^0 = 0$ and strong coupling ($\beta = 1$) where the damping tends to a constant value asymptotically. The splitting

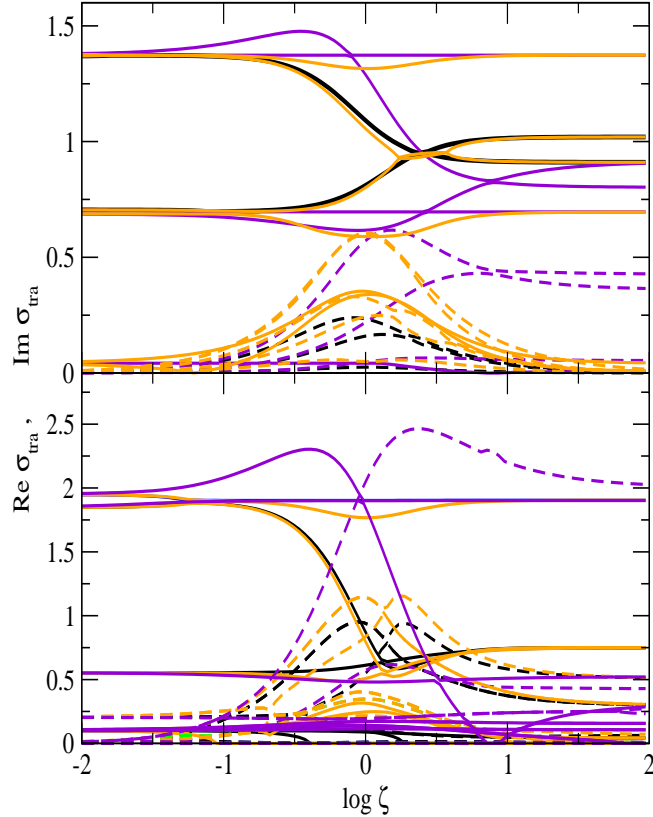


FIG. 2: The second order transverse shear ($l = 2$ m = 1) modes as functions of the drag-to-lift ratio $\log \zeta$.

The black (heavy) and the orange (medium-light) lines correspond to inviscid limit and $\alpha^0 = 0$ and $\alpha^0 = \infty$ cases, respectively. The green (light) lines show the modes in the viscous case with $\alpha^0 = 0$. The conventions are the same as in Fig. 1

of the modes is twice the rotation frequency in the weak coupling regime and is proportional to α^0 in the strong coupling regime, where α^0 is defined via the relation $\alpha^0 = (1 + \alpha^0)^0$, i.e. reflects the mismatch in the volume of the normal uid and super uid. The damping of the modes is negligible in the limits of both large and small α^0 (except $\alpha^0 = \infty$ and $\alpha^0 = 1$ limit) and is maximal for $\alpha^0 = 1$. This feature is generic to the damping of all modes and is a result of low vortex mobility for motions away or towards the spin axis. In the small limit the lattice moves with the super uid while in the large limit it is locked to the normal uid. Comparing the modes for the slow and fast rotation cases (upper and lower panels of Fig.

2) we see that the modes in the fast rotation regime show the same basic features of the slow rotations with a few exceptions: (i) first, the splittings of the real parts of the modes are magnified in the strong and weak coupling limits, which is qualitatively consistent with the scalings with discussed above; (ii) the two high-frequency modes are non-oscillatory in the crossover region 1.

When the viscosity of the normal fluid is taken into account, the number of modes double, because now the relative and center-of-mass modes mix. The solutions of the twelfth order characteristic equation for the transverse shear modes in the case of viscous thermal cloud are shown in Fig. 2 by green (light) lines. The value of the kinematic viscosity is fixed at $\nu = 2$; (we note here that the parameter ν is not small in our examples below, and the perturbation expansion for the relative modes breaks down for $\nu = 1$. The quoted value was chosen to make the differences between the inviscid and viscous case visible on the scale of the figure).

The solutions to the secular equations for the modes appear as complex conjugates (reflecting the axial symmetry of the problem), i.e., there are six distinct solutions for the transverse-shear modes (some of the modes are indistinguishable on the scale of the figure). Consistent with the perturbative treatment of the viscosity effects a subset of modes in Fig. 2 shows only small deviations from the inviscid case, mostly in the crossover region between the strong and weak couplings ($\nu = 1$). The remainder modes are almost independent of the mutual friction and are associated with the center-of-mass oscillations modes. The generic features of the relative oscillation modes are unchanged when viscosity is included (the mode-crossing, asymptotic splittings of the real parts and the asymptotic decay of the imaginary parts). The shift in the position of the crossing point compared to the inviscid and $\nu = 0$ case is due to the effective rescaling of the ν^0 parameter by the term s / f_s . Note that the damping of the center-of-mass modes is solely due to the viscosity and the bell-shaped imaginary parts seen in Fig. 2 are the consequence of our assumption that $s / f_s \ll 1$; (assigning a constant value to the kinematic viscosity would not change the qualitative picture above, but would render the damping of the center-of-mass oscillations independent of s / f_s).

The solutions of the fourth order characteristic equation for the toroidal modes ($l = 2, m = 0$) are displayed in Fig. 3. Conventions are the same as in Fig. 2. Only two distinct solutions exist in the inviscid limit, since the modes appear as complex conjugates due to the axial symmetry of the problem. An inspection of Fig. 3 shows that the basic qualitative

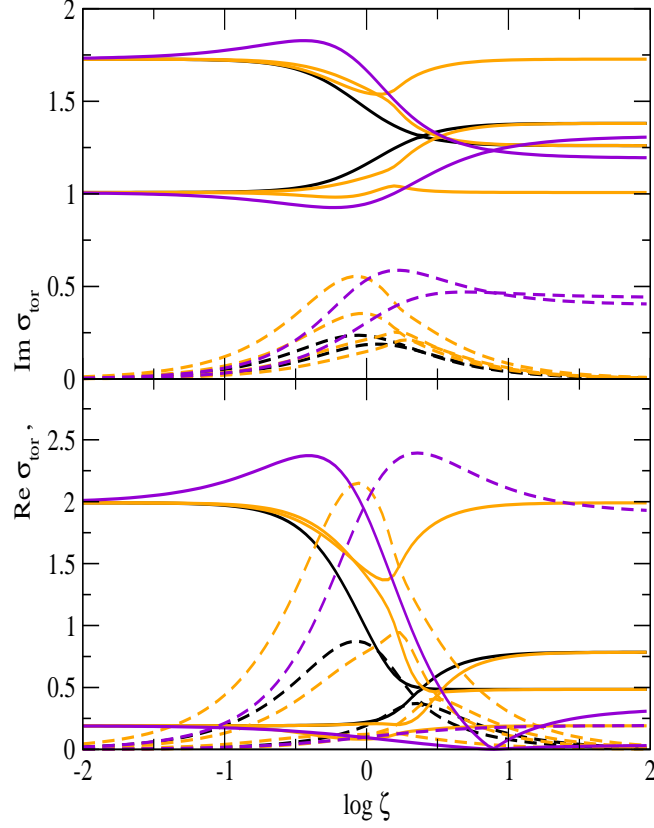


FIG . 3: The second order toroidal ($l = 2$ $m = 2$) modes as functions of the drag-to-lift ratio $\log \zeta$. The conventions are the same as in Fig. 2.

features of the toroidal modes are the same as those of the transverse-shear modes, although there are some quantitative differences. We briefly list these features: (i) the pair of solutions degenerate to a single value (mode-crossing) for $\zeta^0 = 1$ in the inviscid and $\zeta^0 = 0$ limits, since then Eqs. (48) and (49) become identical. (ii) For $\zeta^0 = 0$ the value of ζ at which the crossing occurs shifts to larger values. (iii) The real parts of the modes are asymptotically constant; the two imaginary parts decay asymptotically to zero and are maximal at $\log \zeta = 0$ and at the mode-crossing point, respectively. (iv) For $\zeta^0 = 0$ the imaginary parts are constants in the limit $\zeta \rightarrow 1$. Quantitatively, the asymptotic values of the frequencies of the toroidal modes are shifted to larger values compared to those of the transverse-shear modes. When the viscosity of the thermal cloud is included, the qualitative new feature is the mixing

of the modes which lead to the doubling of the number of distinct toroidal modes. The additional modes can be attributed to the center-of-mass oscillations. The validity of the perturbative treatment of viscous effects is justified, since the deviations of the modes from the inviscid case are seen to be small for slow rotation case. (In the case of the fast rotation the deviations from the inviscid limit are large and the perturbation expansion breaks down in the crossover region $\beta \approx 1$).

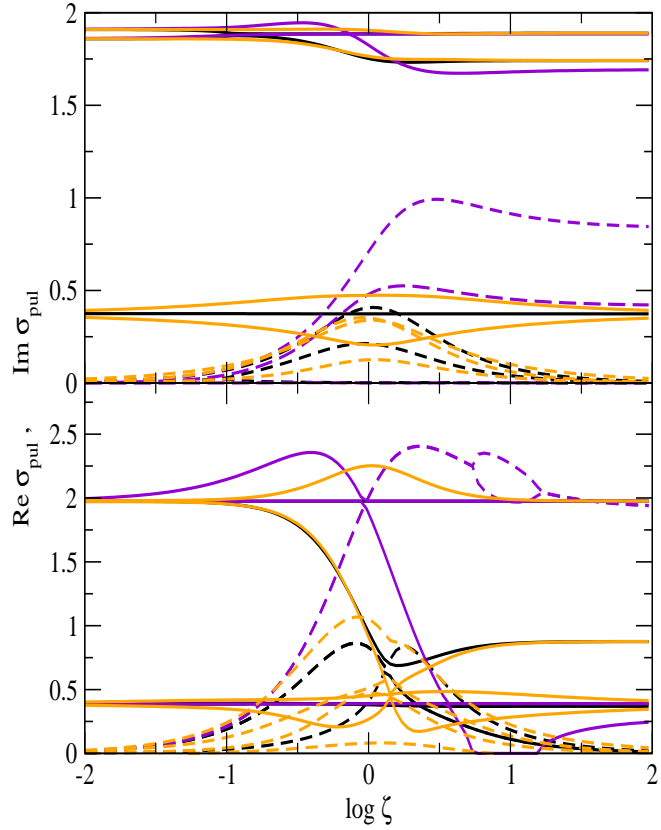


FIG. 4: The second order pulsation ($l=2 m=0$) modes as functions of the drag-to-lift ratio $\log \zeta$. The conventions are the same as in Fig. 2.

Fig. 4 displays the real and imaginary parts of the pulsation ($l=2 m=0$) modes. The distinctive feature of the pulsation modes is that the in-phase and out-of-phase oscillations mix even in the inviscid limit because pressure perturbations for the normal gas and the condensate are governed by different adiabatic indices. The ninth order secular equation for the

pulsation modes has four distinct solutions plus a zero-frequency mode (as before, because of the axial symmetry the modes appear as complex conjugates). Unlike the modes with $m \neq 0$ there is no crossing for the pulsation modes when $\epsilon = 0$, but the two high-frequency modes, that can be associated with the out-of-phase oscillations, cross for $\epsilon \neq 0$. The two low-frequency modes are almost indistinguishable from each other and are weakly affected by the mutual friction (at the second decimal value); these can be associated with the center-of-mass motions. Symptotically, the real parts of the modes are constants. The functional dependence of the damping on the friction is the same as that of the toroidal and transverse-shear modes. Including the viscosity of the thermal cloud causes small modifications in the relative (high-frequency) oscillation modes; the splitting among the center-of-mass oscillation modes significantly increases with a maximum at $\log \Omega = 1$. The case of the fast rotations (lower panel of Fig. 4) reveals a number of interesting features: (i) the asymptotic values of the three of the modes is hardly affected by the change in the spin-frequency, while the real part of a relative oscillation mode drops to zero in the interval $0.7 \leq \log \Omega \leq 1.2$ for $\epsilon = 0$ which gives rise to a bifurcation of the associated imaginary parts into two branches; (ii) in the strong coupling regime the modes are either partially ($\epsilon = 0$) or fully ($\epsilon = 0$) damped. As in the case of the slow rotations the viscosity removes the near degeneracy among the low-frequency modes. The modes are mostly affected in the crossover regime $\log \Omega = 1$ because of our assumption $\epsilon / \Omega \ll 1$.

IV. CONCLUSIONS

In the sections above we have seen that the finite temperature oscillation modes of a harmonically confined rotating Bose-Einstein gas contain rich information on the physics of condensate, the thermal cloud and their interactions via the vortex lattice. Quite generally, the modes separate into two classes corresponding to the in-phase (center-of-mass) and counter-phase (relative) oscillations of the thermal cloud and the condensate. The first class of modes involves oscillations of the combined mass of the cloud and the condensate, and is the analog of the first sound in non-rotating superuids. The second class of modes carries zero net mass-current, involves entropy oscillations of the thermal cloud, and hence, is the analog of the second sound. The two classes of modes are independent in the inviscid limit, with the exception of the radial pulsations, which are coupled due to the difference

in adiabatic pressure perturbations of the cloud and the condensate. If the thermal cloud is viscous, the oscillations involve coupled mass and entropy currents for either classes of modes. Two distinct mechanisms of damping of perturbations from the equilibrium rotating state are operative: the mutual friction between the condensate and the thermal cloud, mediated by the vortex lattice, damps the second class of out-of-phase oscillations. The kinematic viscosity damps the first class of in-phase oscillations of the thermal cloud and the condensate. When the two classes of modes are coupled, the kinematic viscosity changes the magnitudes of the damping rates of the relative oscillation modes.

Unlike the zero-temperature case, where the lowest order non-trivial (i.e. different from ordinary rotation) modes of oscillations belong to the second order ($l=2$; $j \neq 2$) harmonics, at finite temperatures the first order harmonic oscillations become non-trivial. These modes represent counter-phase oscillations of the thermal cloud and the condensate and are simple enough to permit analytical description [Eqs. (39) and (40)]. The analysis above shows that an experimental observation of deviations of the eigen-modes of the odd-parity oscillations from ω_k and/or their damping will indicate non-zero friction orthogonal to the equatorial plane, which could be caused by convective motions or vortex bending. Mapping out experimentally the dependence of the even parity modes on the rotation frequency and the lift-to-drag ratios can potentially pin down the values of macro- and microscopic parameters. For example, locating the crossing point of the two eigen-modes would fix the value of the β -parameter, provided the force component proportional to β^0 is negligible. Measuring in addition the position of the centroid around which the modes are split in the strong coupling regime ($\beta \gg 1$) could fix both β and β^0 parameters. The magnitude of the splitting in the strong coupling regime, on the other hand, provides information on the parameter $\beta = \frac{f_c}{f_N}$, where f_c is the volume filling factor, and $f_{c,N}$ are the fractional densities of the condensate and the cloud.

The drag-to-lift ratios depend on the elementary processes of quasi-particle/vortex scattering, the strength of the interparticle interactions, and on thermodynamic parameters, such as the density and the temperature. A possible scenario of mapping out the dependence of the modes on the mutual friction parameters could involve tuning the interparticle interactions in the vicinity of a Feshbach resonance and sizably changing the quasi-particle/vortex scattering cross-section by small variations in the magnetic field. Varying the thermodynamic parameters, for example, the temperature of the system is another possibility. If the

system is prepared such (or the bosonic species are chosen such) that the strong coupling regime is operative, measuring the relative oscillations modes at various spin frequencies can provide information on the actual values of the mutual friction and related parameters. The mutual friction coefficients can also be fixed by measuring the damping of the modes. Quite generally, the damping is asymptotically negligible in the weak ($\beta = 1$) and strong ($\beta = 0$) coupling limits except when $\beta = 0$ and $\beta \neq 1$, in which case the damping is constant asymptotically. The damping is maximal in the crossover regime between the weak and strong coupling at $\log \beta = 0$ and $\log \beta = 0.4$ (for $\beta = 0$) depending on the mode.

The second order harmonic modes of oscillations are more complex, since they involve a larger number of modes and the in- and out-of-phase oscillations can not be disentangled in a number of cases. Nevertheless, the properties of the relative transverse-shear ($m = 1$) and toroidal ($m = 2$) modes are to a large extent analogous to those of the first order modes. There is a mode crossing for the two high-frequency modes defined by the condition $\beta \approx 1$. The real parts are asymptotically constant and the imaginary parts tend to zero; exception is the case $\beta = 0$ and $\beta \neq 1$ where the imaginary parts tend to constants. The bell-shaped form of the imaginary parts with maxima at $\log \beta = 0$ and $\log \beta = 0.4$ (for $\beta = 0$) is generic to the relative transverse-shear ($m = 1$) and toroidal ($m = 2$) modes as well. In the fast rotation limit the damping of the modes is enhanced, since the dissipative terms in the virial equations scale linearly with the spin frequency. Likewise, the asymptotic splitting of the eigen-modes in the strong and weak coupling limits is enhanced linearly in β . The distinctive feature of the second order harmonic pulsation modes ($m = 0$) is that they couple the in- and out-of-phase oscillations even when the viscosity of the matter is negligible. There is no mode crossing for the pulsation modes (for the common case $\beta = 0$) and the decay rates have their maxima at $\beta = 0$ only.

Experimental studies of the dependence of the second order harmonic modes on the lift-to-drag ratios and the variations of the spin-frequency can potentially some of the parameters reflecting the micro-physics of quasi-particle-vortex interactions. In addition, information can be obtained on the magnitude of the kinematic viscosity from the damping or splitting of the eigen-frequencies of the center-of-mass modes. It should be kept in mind that Eqs. (1)–(4) for the center-of-mass modes remain valid at finite temperatures whenever the in- and out-of-phase oscillations are uncoupled.

The method described above could be applied to superuid Fermi-systems at finite tem-

peratures with minor modifications. For Fermi-superuids which rotate as a rigid body and are confined by a harmonic trap, the oscillation modes will differ from those described above to the extent the equations of states of the normal and superuid differ from those of a Bose-gas. Since the linearized perturbation equations involve pressure perturbations only for the pulsation modes, the remainder oscillations would be identical to those described above. The pulsation modes can be easily handled by using an appropriate adiabatic index for a Fermi-superuid at finite temperatures.

Appendix: Small amplitude oscillations in nonaxisymmetric traps

Here, for completeness, we list the linearized virial equations appropriate for finding the modes of rotating confined Bose-Einstein gas in anisotropic traps. We do not attempt numerical solutions of these equations, since it is clear from the analysis of the axisymmetric modes that the system supports large number of modes which would not be easy to disentangle in an experiment. Lifting the axial symmetry, will remove the degeneracy of the modes seen in the axially symmetric case and thus will increase the number of modes further. As in the case of axisymmetry, the modes can be separated into two subsets which have even and odd parities with respect to the direction of the rotation axis and we shall list them separately.

Even parity modes

The even parity modes are determined by the components of Eqs. (46) and (47) which are even in index 3, i.e. involve the combinations $i; j = (11), (22), (21), (12)$ and (33) . This set of equations can be manipulated in a manner that excludes the variations of the pressure tensor; convenient combinations are $(11) - (22)$, $(11) + (22) - 2(33)$, $(12) - (21)$ and $(12) + (21)$. For the center-of-mass virials this set reads

$$\begin{aligned}
 & \frac{2}{2} + \text{if}_N + !_1^2 \quad !^2 V_{11} \quad \frac{2}{2} + \text{if}_N \frac{a_2^2}{a_1^2} + !_2^2 \quad !^2 V_{22} \quad 2i \quad V_{12} \\
 & \text{if}_N f_S \quad U_{11} + \text{if}_N f_S \frac{a_1^2}{a_2^2} U_{22} = 0; \\
 & \frac{2}{2} + \text{if}_N + !_1^2 \quad !^2 V_{11} + \frac{2}{2} + \text{if}_N \frac{a_1^2}{a_2^2} + !_2^2 \quad !^2 V_{22}
 \end{aligned} \tag{93}$$

$$\begin{aligned}
& 2 + 2!_3^2 - 2\text{if}_N \frac{a_1^2}{a_3^2} V_{33} + 2i (V_{1,2} - V_{2,1}) \\
& \text{if}_N f_S U_{11} - \text{if}_N f_S \frac{a_1^2}{a_2^2} U_{22} + 2\text{if}_N f_S \frac{a_1^2}{a_3^2} U_{33} = 0; \\
& (94)
\end{aligned}$$

$$2 (V_{1,2} - V_{2,1}) - i (V_{11} + V_{22}) + (!_1^2 - !_2^2) V_{12} = 0;$$

$$\begin{aligned}
& " \\
& 2 + \text{if}_N 1 + \frac{a_1^2}{a_2^2} V_{12} + i (V_{11} + V_{22}) - \text{if}_N 1 \frac{a_1^2}{a_2^2} (V_{1,2} - V_{2,1}) \\
& \text{if}_N f_S 1 + \frac{a_1^2}{a_2^2} U_{12} + \text{if}_N f_S 1 \frac{a_1^2}{a_2^2} (U_{1,2} - U_{2,1}) = 0; \\
& (96)
\end{aligned}$$

For the virials corresponding to the relative motions the same combination of the components of the Eq. (47) reads

$$\begin{aligned}
& \frac{2}{2} + i \sim + \text{if}_S + !_1^2 - 2 U_{11} - \frac{2}{2} + i \sim + \text{if}_S + !_2^2 - 2 U_{22} \\
& 2i (1 - \sim^0) U_{12} - i V_1 + i V_{22} = 0; \\
& \frac{2}{2} + \text{if}_S + !_1^2 - 2 U_{11} + \frac{2}{2} + \text{if}_S \frac{a_1^2}{a_2^2} + !_2^2 - 2 U_{22} \\
& 2 + 2i \sim^0 + 2\text{if}_S \frac{a_1^2}{a_3^2} + 2!_3^2 U_{33} + 2i (1 - \sim^0) (U_{1,2} - U_{2,1}) \\
& i V_1 - i \frac{a_1^2}{a_2^2} V_{22} + 2i \frac{a_1^2}{a_3^2} V_{33} = 0; \\
& (97)
\end{aligned}$$

$$(2 + 2i \sim) (U_{1,2} - U_{2,1}) - i (1 - \sim^0) (U_{11} + U_{22}) + (!_1^2 - !_2^2) U_{12} = 0;$$

$$\begin{aligned}
& " \\
& 2 + 2i \sim + \text{if}_S 1 + \frac{a_1^2}{a_2^2} + !_1^2 + !_2^2 - 2 U_{12} + i (1 - \sim^0) (U_{11} + U_{22}) \\
& \text{if}_S 1 + \frac{a_1^2}{a_2^2} (U_{1,2} - U_{2,1}) - i 1 + \frac{a_1^2}{a_2^2} V_{12} + i 1 \frac{a_1^2}{a_2^2} (V_{1,2} - V_{2,1}) = 0; \\
& (100)
\end{aligned}$$

Odd parity modes

The components of Eqs. (46) and (47) which are odd in index 3 involve the combinations $i, j = (13), (23), (31), (32)$. By suitably combining these components we find for the center-of-mass virials the following set of equations

$$\begin{aligned} & \text{if}_N \quad 1 \quad \frac{a_1^2}{a_3^3} \quad V_{1;3} \quad 2i \quad V_{2;3} + \frac{!_1^2}{!_1^2} \quad ^2 + \text{if}_N \quad V_{13} \\ & \quad + \text{if}_N f_S \quad 1 \quad \frac{a_1^2}{a_3^3} \quad U_{1;3} \quad \text{if}_N f_S \quad U_{13} = 0; \end{aligned} \quad (101)$$

$$\begin{aligned} & \text{if}_N \quad 1 \quad \frac{a_1^2}{a_2^2} \quad V_{2;3} + 2i \quad V_{1;3} + \frac{!_2^2}{!_2^2} \quad ^2 + \text{if}_N \quad \frac{a_1^2}{a_2^2} \quad V_{23} \\ & \quad \text{if}_N f_S \quad \frac{a_1^2}{a_2^2} \quad \frac{a_1^2}{a_3^2} \quad U_{2;3} \quad \text{if}_N f_S \quad \frac{a_1^2}{a_2^2} \quad U_{23} = 0; \end{aligned} \quad (102)$$

$$\begin{aligned} & \text{if}_N \quad + \frac{!_3^2}{!_3^2} \quad V_{13} \quad ^2 + \text{if}_N \quad 1 \quad \frac{a_1^2}{a_2^2} \quad V_{1;3} \\ & \quad + \text{if}_N f_S \quad 1 + \frac{a_1^2}{a_3^2} \quad U_{1;3} \quad \text{if}_N f_S \quad U_{13} = 0; \end{aligned} \quad (103)$$

$$\begin{aligned} & \text{if}_N \quad \frac{a_1^2}{a_2^2} \quad + \frac{!_3^2}{!_3^2} \quad V_{23} \quad ^2 + f_N \quad \frac{a_1^2}{a_3^2} \quad \frac{a_1^2}{a_2^2} \quad V_{2;3} \\ & \quad \text{if}_N f_S \quad \frac{a_1^2}{a_3^2} \quad \frac{a_1^2}{a_2^2} \quad U_{1;3} \quad \text{if}_N f_S \quad \frac{a_1^2}{a_2^2} \quad U_{13} = 0; \end{aligned} \quad (104)$$

By a similar reduction the components of Eq. (47) can be reduced to

$$\begin{aligned} & \text{if}_S \quad 1 \quad \frac{a_1^2}{a_3^3} \quad U_{1;3} \quad 2i \quad (1 \quad 0) \quad U_{2;3} + \frac{!_1^2}{!_1^2} \quad ^2 + \text{if}_S \quad U_{13} \\ & \quad + i \quad 1 \quad \frac{a_1^2}{a_3^3} \quad V_{1;3} \quad i \quad V_3 = 0; \end{aligned} \quad (105)$$

$$\begin{aligned} & \text{if}_S \quad \frac{a_1^2}{a_3^2} \quad \frac{a_1^2}{a_2^2} \quad U_{2;3} + 2i \quad (1 \quad 0) \quad U_{1;3} + \frac{!_2^2}{!_2^2} \quad ^2 + \text{if}_S \quad \frac{a_1^2}{a_2^2} \quad U_{23} \\ & \quad i \quad \frac{a_1^2}{a_3^2} \quad \frac{a_1^2}{a_2^2} \quad V_{2;3} \quad i \quad \frac{a_1^2}{a_2^2} \quad V_{23} = 0; \end{aligned} \quad (106)$$

$$+ i \frac{a_1^2}{a_3^2} V_{1,3} - i V_3 = 0; \quad (107)$$

$$^2 + 2i \frac{a_1^2}{a_2^2} + i f_s \frac{a_1^2}{a_2^2} + !^2_3 U_{23} = 0; \quad (108)$$

$$^2 + 2i \frac{a_1^2}{a_3^2} + i f_s \frac{a_1^2}{a_3^2} \frac{a_1^2}{a_2^2} U_{2,3} = 0;$$

$$+ i \frac{a_1^2}{a_2^2} \frac{a_1^2}{a_3^2} U_{1,3} - i \frac{a_1^2}{a_2^2} V_{23} = 0;$$

[1] K.W. Madison, F. Chevy, W. Wohlleben, and J. Dalibard, *Phys. Rev. Lett.* **84**, 806 (2000).

[2] J.R. Abo-Shaeer, C. Raman, W. Ketterle, *Phys. Rev. Lett.* **88**, 070409 (2002).

[3] C. Raman, J.R. Abo-Shaeer, J.M. Vogels, K. Xu, W. Ketterle, *Phys. Rev. Lett.* **87**, 210402 (2001).

[4] P.C. Haljan, I. Coddington, P. Engels, E.A. Cornell, *Phys. Rev. Lett.* **87**, 210403 (2001).

[5] S. Chandrasekhar, *Ellipsoidal Figures of Equilibrium* (Yale University Press, New Haven, 1969).

[6] A. Sedrakian and I. Wasserman, *Phys. Rev. A* **63**, 063605 (2001) (Paper I).

[7] M. Cozzini and S. Stringari, *Phys. Rev. A* **67**, 041602 (2003).

[8] F. Chevy and S. Stringari, cond-mat/030559.

[9] I.M. Khalatnikov, *Introduction to the Theory of Superfluidity* (Addison Wesley, New York, 1989).

[10] C.J. Pethick and H. Smith, *Bose-Einstein Condensation in Dilute Gases* (Cambridge University Press, Cambridge, 2002).